# Bulk Defects and Hydrogenation Kinetics in Fired Passivating Contacts

Mario Lehmann[a], Anatole Desthieux[b,c,d], Nathalie Valle[e], Audrey Morisset[a], Philippe Wyss[a], Santhana Eswara[f], Tom Wirtz[f], Andrea Ingenito[g], Pere Roca i Cabarrocas[b,d], Christophe Ballif[a,g], Franz-Josef Haug[a,*]

[a] *Ecole Polytechnique Fédérale de Lausanne (EPFL), Institute of Electrical and Micro Engineering (IEM), Photovoltaics and Thin Film Electronics Laboratory, Rue de la Maladière 71b, 2002 Neuchâtel, Switzerland*

[b] *Institut Photovoltaïque d'Ile de France (IPVF), 18 Boulevard Thomas Gobert, 91120 Palaiseau, France*

[c] *EDF R&D, Bvd Gaspard Monge, 91120 Palaiseau, France*

[d] *LPICM, CNRS, Ecole Polytechnique, Institut Polytechnique de Paris, route de Saclay, 91128 Palaiseau, France*

[e] *Advanced Characterization Platform (ACP), Luxembourg Institute of Science and Technology (LIST), Materials Research and Technology Department, 41, rue du Brill, L-4422 Belvaux, Luxembourg*

[f] *Advanced Instrumentation for Nano-Analytics (AINA), Luxembourg Institute of Science and Technology (LIST), Materials Research and Technology Department, 41, rue du Brill, L-4422 Belvaux, Luxembourg*

[g] *CSEM PV-Center, Jaquet-Droz 1, 2002 Neuchâtel, Switzerland*

** Corresponding author: franz-josef.haug@epfl.ch*

**Keywords**

Passivating contacts, silicon solar cells, bulk defects, hydrogenation, kinetics, float-zone, MPL, SIMS

## ABSTRACT

In this work, the effect of the various processing steps during the fabrication of c-Si/$SiO_x$/$SiC_x$ fired passivating contacts on the silicon bulk lifetime is studied, and the kinetics of defect deactivation by hydrogenation investigated. It is found that the firing step at 800 °C induces shallow bulk defects in Float-Zone (FZ) silicon wafers, which can subsequently be passivated with hydrogen provided by an a-$SiN_x$:H/D reservoir layer upon annealing at 450 °C. Experimental results and numerical data treatment indicate a rapid passivation of the surface within less than 1 min, followed by a slower passivation of the shallow bulk defects. *In situ* lifetime measurements are consistent with a slow bulk lifetime improvement by showing similar lifetime evolutions for both p-type and n-type $SiC_x$ layers. The kinetics of the hydrogenation process seems to be limited by the available hydrogen supply at the c-Si/$SiO_x$ interface, rather than by its diffusion within the bulk of the wafer. Moreover, it is affected by the bulk doping, as well as the $SiC_x$ layer thickness. Finally, it is shown that hydrogenation is also possible with an a-$SiN_x$:H/D reservoir layer deposited on one side of the wafer only, although resulting in a lower passivation level ($\tau_{eff}$ ~700 µs

compared to $\tau_{eff}$ ~1300 µs for symmetrical samples), and slower kinetics ($\tau_{reac}$ ~5 min compared to $\tau_{reac}$ ~0.8 min).

## 1. INTRODUCTION

Full area passivating contacts resisting high temperature treatments attracted a lot of attention in the past years. Their integration in c-Si solar cells has recently enabled to reach conversion efficiencies above 26% [1], [2] and first industrial production lines to fabricate cells featuring such contacts are currently being ramped up [3]–[5]. Such contacts typically consist of a thin (1.2-3.6 nm) silicon oxide ($SiO_x$) layer, capped with a doped poly-silicon layer (poly-Si), that subsequently undergo a high-temperature treatment and a hydrogenation step. Lately, a special focus has been put on the so-called firing step, which is a rapid high-temperature process used to form the screen-printed metallization, commonly used in industrial mass production. Compatibility of the passivating contacts with this process is crucial for a straightforward transfer of the technology from laboratories to industry [6]. On the one hand, this firing process has been reported to damage the sample's passivation [7]–[9], while on the other hand it has been investigated as a low thermal budget approach to form Fired Passivating Contacts (FPC) [10], [11]. The kinetics of the hydrogenation process has also been studied in more detail recently, providing further insight on the mechanisms at work and the factors limiting the passivation. Dingemans et al. investigated it in the case of hydrogen diffusing from $Al_2O_3$ layers deposited on c-Si/$SiO_2$ stacks [12], and Polzin et al. for various hydrogenation approaches for their TOPCon architecture [13].

In this work, the evolution of the silicon bulk lifetime upon firing and hydrogenation is investigated, in order to discriminate between effective lifetime changes due to bulk or surface passivation variations and complement the findings of our previous study, where the impact of various processing steps on the hydrogen distribution near the surface was investigated [14]. As the final goal was to assess the surface passivation quality provided by FPCs, FZ wafers were used. The latter are widely used in research laboratories as FZ silicon is of high purity, resulting in high minority carrier bulk lifetimes [15]–[18]. In the case of the hydrogenation process, its kinetics is investigated, trying again to discriminate between evolution of bulk and surface lifetimes upon diffusion of hydrogen from an a-$SiN_x$:H/D reservoir layer, which was reported to be a key step for good passivation of FPCs [10], [14]. Finally, the diffusion of hydrogen from a front a-$SiN_x$:H/D layer through the whole wafer is investigated to provide additional insight into hydrogenation kinetics, and to test a passivation approach potentially interesting for a cell architecture featuring a p-type passivating contact at the rear side and the hydrogen reservoir in the a-$SiN_x$:H layer doubling as anti-reflective coating on the front.

## 2. EXPERIMENTAL

### 2.1. Fabrication

The samples for the present study were processed on (100) oriented FZ silicon wafers with a Shiny-Etched (SE) or Double Side Polished (DSP) surface finish and a diameter of 10 cm. The SE wafers have a thickness of 200 µm and a resistivity of 2 Ωcm, while the DSP wafers are 280 µm thick and have a resistivity of 3 Ωcm. If not stated otherwise, they were boron-doped (p-type). The sample fabrication started with a chemical cleaning. Next, a $SiO_x$ layer was grown at the surface. This was done either chemically ($HNO_3$, 69%, 80 °C, 10 min) [19], [20], or by exposing the wafer to UV radiation in ambient air (2-3 min each side), leading to the formation of $O_3$ oxidizing the silicon surface [21]–[23], both resulting in a ~1.3 nm thin tunneling oxide, or thermally (90 min at 900 °C in an oxygen ambient)

[24]–[27], resulting in a ~25 nm thick oxide. A 10-40 nm thick hydrogenated amorphous a-$SiC_x$ layer (~2.5 at.% of carbon [10]) was then deposited by Plasma Enhanced Chemical Vapor Deposition (PECVD), using $SiH_4$, $H_2$, $CH_4$, $PH_3$ (n-doped layers) and $B(CH_3)_3$ (p-doped layers) precursor gases. These depositions were performed in two similar tools, called Kai-M and Octopus. The samples were then fired for 3 s at 800 °C, crystallizing the previously amorphous layers into nano-crystalline nc-$SiC_x$[1] and effusing most of the hydrogen contained in the layer after deposition, as reported previously [14]. Finally, the samples were hydrogenated. To do so, a ~70 nm thick a-$SiN_x$:H/D layer was deposited by PECVD at 250 °C on one or both sides of the wafers, releasing hydrogen during a subsequent hotplate anneal at 450 °C for 30 min [28]. Deuterium was incorporated into the a-$SiN_x$:H/D layers by replacing the $H_2$ gas flow by $D_2$ in the PECVD process. In some cases, the a-$SiN_x$:H/D layer was removed after hydrogenation by dipping the samples in a 5% HF solution for 12 min. The fabrication process is schematically represented in Fig. 1.

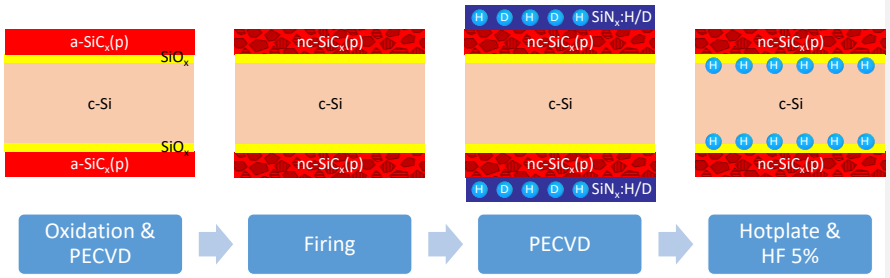


**Fig. 1**: Schematic illustration of the fabrication process using a sacrificial a-$SiN_x$:H/D layer for hydrogenation. Note that a chemical cleaning was performed prior to the oxidation.

### 2.2. Characterization

To assess the passivation quality of the fabricated samples, Quasi-Steady-State Photoconductance (QSSPC) measurements and photoluminescence (PL) imaging were performed. QSSPC was measured using a Sinton WCT-120 instrument, providing the effective minority carrier lifetime ($\tau_{eff}$) as function of the minority carrier density (MCD), as well as the implied open circuit voltage ($iV_{OC}$) at 1 sun [29]–[31], implementing the Auger correction published by Richter et al [32]. As for PL imaging, it was measured with an in-house built setup. The samples are excited using an Ostech laser with a wavelength of 808 nm, operated with a power of 1.2 suns, and the images are recorded with a PIXIS Princeton instrument silicon-based camera.

*In situ* Modulated Photoluminescence (MPL) was used to track the evolution of the minority carrier lifetime in real time during the hydrogen diffusion step at 450 °C. In this setup, it is determined through the measurement of the phase-shift between the modulated laser illumination and the photoluminescence signal, as described by Desthieux et al. [33].

The chemical composition of some samples was measured by Secondary Ion Mass Spectrometry (SIMS), using a CAMECA SC-Ultra instrument with a 1 keV $Cs^+$ primary ions bombardment. Oxygen, hydrogen and deuterium were analyzed as $MCs^+$ ions, collected from an area of 60 µm in diameter, with a depth resolution of ~4 nm (not element dependent) [34].

[1] Based on transmission electron microscopy observations, we assume this layer to be formed of nc-Si grains in an a-$SiC_x$ matrix [66].

## 3. RESULTS & DISCUSSION

### 3.1. Shallow bulk defects created upon firing

In order to assess the evolution of the bulk lifetime during the processing sequence, the deposited layers were removed from samples at various stages of the process, using HF to etch off a-SiN$_x$:H/D and CP4[2] to etch off nc-SiC$_x$. Subsequently, their surfaces were coated with amorphous silicon layers, providing excellent surface passivation [35]. Doing so allows to observe bulk defects, as in their presence the measured effective lifetime becomes bulk limited. As can be seen in Fig. 2, a ring shape appears after firing, indicating that bulk defects have been created [36]. These bulk defects can be passivated by hydrogen, as suggested by Fig. 2c and more clearly by Fig. 4 below. Hiller et al. and de Guzman et al. reported similar findings, using FZ wafers too, and they proposed that the defect could be due to Si-vacancies that capture N-atoms, leading to dangling bonds that can be passivated with hydrogen [15], [37]. The reason why the sample in Fig. 2c, that underwent a hydrogenation process, still displays some ring shape, is believed to be hydrogen effusion during the heating phase of the PECVD process prior to the deposition of the a-Si:H layers (200 °C under vacuum for 7 min without any capping layer).

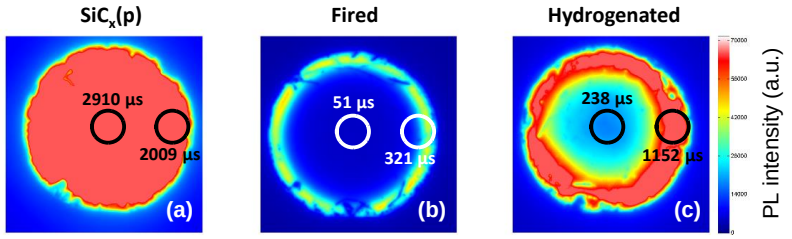


**Fig. 2**: PL images of samples at different processing stages which layers have been etched off by HF and CP4 and the surface repassivated using a-Si:H(i)/a-Si:H(n) stacks. Sample (a) has been etched and repassivated directly after PECVD of a-SiC$_x$(p) layers, sample (b) after subsequent firing for 3 s at 800°C, sample (c) after subsequent hydrogenation by H-diffusion from an a-SiN$_x$:H/D reservoir layer.

In order to gain further insight into the defect properties, lifetime measurements were performed at various temperatures, ranging from 25 °C to 190 °C, on hydrogenated samples still capped with a-SiN$_x$:H/D layers. Following the approach proposed by Murphy et al. [38], we find that the dominating limitation is a shallow bulk defect, as indicated by the negative slope of the linear region at high injection in Fig. 3a. Expressing this region through $\tau = a + b \cdot x$, extrapolation to $x \to 1$ yields the ambipolar lifetime $\tau_{amb} = a + b$, and the ratio $\xi$ defined by $\xi = b/(a + b)$ yields a quantity that is characteristic for the defect, but independent of its concentration [38], [39]. The two fitting parameters $a$ and $b$ do not uniquely determine the properties of the defect, but they can be used to obtain a functional dependence between the ratio of the capture cross sections, $k$, and the defect energy $E_t$ which is called Defect Parameter Solution Surface (DPSS). Thus, $k = -(p_1/\, p_0 + \xi)/(\xi - 1 + n_1/p_0)$ where $p_0$ is the doping concentration of the wafer and $p_1$, and $n_1$ are the parameters defined in the Shockley-Read-Hall (SRH) statistics [40], [41].

As the DPSS for the lifetime curves measured at various temperatures should intersect at the most likely values of $E_t$ and $k$ [42], Fig. 3b indicates that the energy level of the defect

[2] Chemical Polish: mixture of HF (50%), $HNO_3$ (69%) and Acetic acid (99.9%), in volume ratios of 10%, 73% and 17%, respectively.



**Commented [LMJ1]:** Andrea Ingenito: In this section would it be possible to make a figure similar to 2 and 3 also samples that have a thermal oxidation? This would allow you to see the impact of a re-annealing

**Commented [LMJ2R1]:** We have some preliminary results, but not enough for a clear story:
Fig. 2: HT803: bulk < 150 us after 30 min at 900°C, not 90 min as for thermal oxide…
Fig. 3: we don't have T-dependent QSSPC measurements on samples with therm. SiO2
→ Since I don't have time for more experiments, I would suggest to leave the manuscript like this.

**Commented [LMJ3]:** Pere Roca: Just a comment here
Do you think the H from the bulk of the wafer does move out at 200 °C ? and even it was the case, should not the hydrogen go in again once you start the capping process ?

**Commented [LMJ4R3]:** Yes, we observed lifetime losses when putting uncapped samples on the hotplate, starting at temperatures around 200-300°C.
However, hydrogen diffusion from a SiNx:H reservoir layer seems to start only at 425°C. So I guess that 200°C is not enough to recover the passivation losses by diffusing H from the a-SiCx:H layer being deposited.

**Commented [LMJ5]:** HT742

should be very close to either the conduction band or the valence band. After subtraction of the contribution of the shallow bulk defect, a residual about an order of magnitude higher than the original lifetime curves is obtained (Fig. 3c), meaning that our passivation after hydrogenation is mainly limited by these shallow bulk defects, and not by recombinations at the c-Si/$SiO_x$ interface as assumed so far (note that above $\Delta n = 2 \times 10^{15}$ $cm^{-3}$ the calculation of the residual is no longer trustworthy, hence the characteristics are shaded). This is a major finding, as it implies that the surface passivation of the present FPCs is much better than expected, and future work should focus on the passivation of bulk defects in order to further increase the minority carrier lifetime.

In our previous study, it was shown that the effective lifetime of the samples stays low until the hydrogenation step is performed [14]. In the light of the results above, it can be concluded that in the as-deposited state, a low surface passivation is the limiting factor. After firing, both bulk and surface lifetime are low, and finally improve upon hydrogenation, with the bulk lifetime becoming the limiting one.

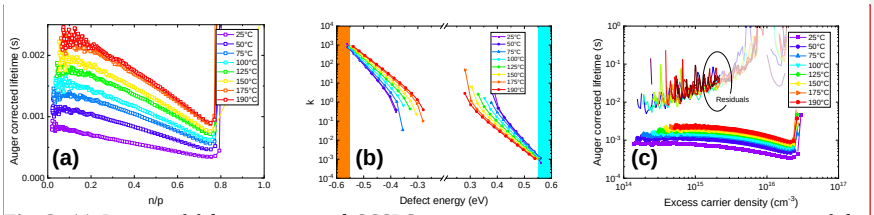


**Fig. 3**: (a) Linearized lifetime curves of QSSPC measurements at various stage temperatures and fits indicating shallow defects. (b) DPSS curves of the same samples. (c) Original lifetime curves and residuals after subtraction of Auger and shallow bulk contributions.

**Commented [LMJ6]:** Comment Prof. Roca: "Figure 3 is very small. It's a pity. Not easy to see.

**Commented [LMJ7R6]:** Leave like that for now and adjust upon final layout (in the case of a 2-column-layout many figures might need adaptations anyway).

The work performed by Grant et al. [36] and Hiller et al. [15] suggests that these bulk defects can be fully cured by annealing for 30 min at temperatures above 800 °C and to a lesser extent by rapid thermal annealing for 30 s. In our case, we mainly create defects with the fast firing process of 3 s at 800 °C (resulting in $\tau_{eff}$ ~50 µs), and we observe only marginal improvement when increasing the firing temperature up to 930 °C and/or prolonging the dwell time up to 30 sec ($\tau_{eff,\,max}$ = 279 µs, reached with 30 s firing at 860 °C). Moreover, the interfacial tunnel oxides seem to get damaged when moving to such harsh firing conditions. Possibly, a long furnace anneal of the wafers prior to the processing of the passivating contacts (similar to the "tabula rasa" treatment for n-type Cz wafers [43]–[45]) could avoid the formation of the shallow defects. This remains to be investigated and would allow to assess the full potential of the fired passivating contact. Potentially, this annealing of the defects could be integrated with the $POCl_3$ diffusion of an n-type front contact, thus maintaining the advantage of a low thermal budget for the formation of the passivating rear contact.

Further ideas to investigate are the use of nitrogen lean FZ material, which was reported to behave differently [36], or the implementation of FPCs on Cz wafers. Indeed, this ring shape issue seems to be inherent to FZ material as a preliminary test did not show them on Cz wafers after firing. However, the lifetime measured on these Cz samples after firing and a-Si:H(i)/a-Si:H(n) surface passivation stayed below 160 µs ($iV_{OC}$ < 675 mV). On the other hand, $iV_{OC}$ values up to 730 mV have been reported for FPCs on Cz wafers after hydrogenation [46]. Hence, further work is needed to understand the bulk lifetime evolution of Cz material upon firing and hydrogenation.

### 3.2. Hydrogenation kinetics

To investigate the evolution of the bulk and surface passivation during hydrogenation, a symmetrical test sample featuring a tunneling $SiO_x/SiC_x$(p)/a-$SiN_x$:H/D stack was annealed on the hotplate at 450 °C in consecutive steps, and PL images were recorded in between. Fig. 4 shows that the PL intensity improves already after 30 sec in the outer regions of the wafer. As this is likely the region with fewer bulk defects [47]–[49], we conclude that the interface defects are already passivated after this short time. The ensuing improvement of the PL signal over the full wafer is thus related to a gradual passivation of the bulk defects, in agreement with the above finding that the shallow bulk defects are the ones limiting the effective lifetime after hydrogenation. This conclusion is further supported by the fact that for samples hydrogenated for 30 min at 350°C, such a ring shape is visible too (not shown here), indicating that even at such low temperature enough hydrogen was diffused to passivate the interface, but not enough to passivate the bulk.

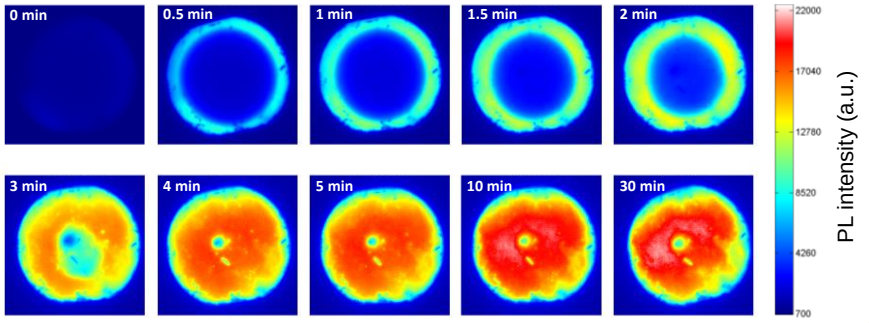


**Fig. 4**: PL images taken at various time intervals during the hydrogenation process by H-diffusion from an a-$SiN_x$:H/D reservoir layer, showing the evolution of the passivation with time spent on the hotplate. The spot with lower PL signal near the center is due to local blistering of the a-$SiN_x$:H/D layer.

In order to allow for a quantitative comparison, the evolution of the passivation was also assessed by measuring the lifetime at regular intervals during the hydrogen diffusion on the hotplate. These curves were then fitted according to $\boldsymbol{\tau_{eff} = [1/\tau_{end} + A \cdot \exp(-t/\tau_{reac})]^{-1}}$, as suggested by Mitchell et al. [50] and Polzin et al. [13], where $\boldsymbol{\tau_{eff}}$ is the measured effective minority carrier lifetime and $\boldsymbol{\tau_{end}}$ and $\boldsymbol{1/\tau_{reac}}$ fitting parameters, corresponding to the minority carrier lifetime reached after hydrogenation and the reaction rate, respectively. Fig. 5 compares the kinetics of samples featuring 1.2 nm thin tunneling $SiO_x$ and 25 nm thick thermal $SiO_2$, as well as n-doped and p-doped $SiC_x$ layers.

The most striking difference in kinetics is between samples with a thermal oxide (saturating within ~1 min, $\tau_{reac}$ < 0.2 min) and those with a tunneling oxide (saturating within ~5 min, $\tau_{reac}$ ~0.8 min). Most likely this is linked to the thermal history of the samples. The tunneling oxides are grown by UV-$O_3$ treatment at room temperature or in $HNO_3$ at 80 °C, whereas the thermal oxide is grown during a 90 min annealing at 900°C, which most likely cured the majority of bulk defects [36]. Thus, we hypothesize that for samples with thick thermal oxide mainly interfacial defects remain to be passivated, leading to a fast hydrogenation process, whereas for samples with tunneling oxide both interfacial and bulk defects remain to be passivated, the latter limiting the kinetics of the hydrogenation process as observed in Fig. 4 above.

Interestingly, no significant difference was observed between samples featuring n-doped and p-doped $SiC_x$ layers, even though the position of the Fermi level was reported to have an influence on the charge-state of hydrogen [51], and hence on its diffusivity [52], [53].

**Commented [LMJ8]:** HT773

This effect can however not be ruled out, as the nc-$SiC_x$(p) layers are thicker and more crystalline than their nc-$SiC_x$(n) counterparts.

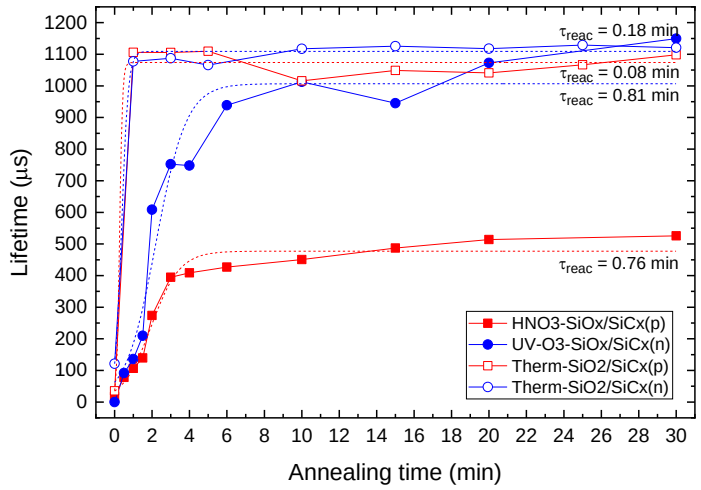


**Fig. 5**: Evolution of effective minority carrier lifetime (at MCD of $\mathbf{1 \cdot 10^{15} cm^{-3}}$) during hydrogenation on hotplate at 450 °C for samples with nc-SiCx(p) or nc-SiCx(n) and ~1.3 nm tunneling $SiO_x$ or ~25 nm thermal $SiO_2$. The dashed lines give the fits according to $\boldsymbol{\tau_{eff} = [1/\tau_{end} + A \cdot \exp(-t/\tau_{reac})]^{-1}}$.

Fig. 5 shows almost instantaneous passivation in the case of thick thermal oxides. In order to slow down the kinetics and to gain further insight in what is speculated to be the hydrogenation of interfacial defects, some samples were annealed on the hotplate at 350 °C rather than 450 °C. The passivation saturates within 5 min, as can be seen in Fig. 6a. In the plot over n/p, the characteristics show a linear behavior only in the as-deposited state and for short treatment times. For longer hydrogenation times, the curvature increases and reaches similar shapes as those hydrogenated at 450°C, shown in Fig. 6b. Since linear behavior is the signature of shallow bulk defects, this trend corroborates the interpretation made earlier, that in the case of samples with a thermal $SiO_2$, the kinetics of the hydrogenation process are limited by the passivation of interfacial defects. Note the the curves in Fig. 6b correspond to open squares in Fig. 5, and display the same behaviour: instantaneous passivation, and a small decrease after 10 min.

**Commented [LMJ9]:** HT736

Commented [LMJ10]: HT644

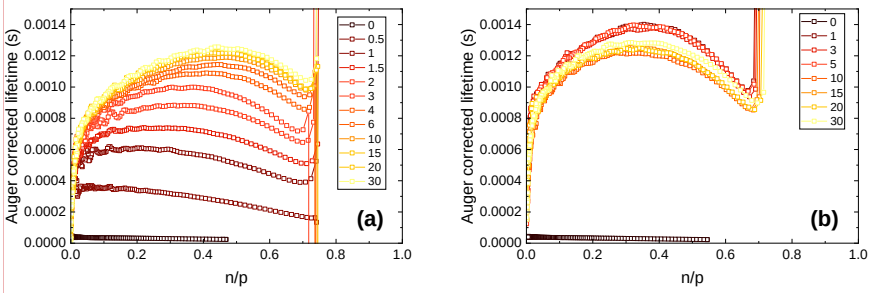


**Fig. 6**: Auger-corrected lifetimes over n/p of samples featuring a thick thermal $SiO_2$ measured at various time steps during the hydrogenation process at 350°C (a) and 450°C (b). The legend gives the total time (in minutes) the sample has spent on the hotplate.

### 3.3. In situ lifetime measurements in real time

So far, all kinetics measurements were performed by annealing the samples shortly on the hotplate in several steps and measuring the effective lifetime at room temperature in between. In order to go one step further and measure the evolution of the lifetime in real time during the hydrogenation process, *in situ* modulated photoluminescence measurements were carried out [33].

First, the evolution of the lifetime in a sample passivated with a $SiO_x$/nc-$SiC_x$(p)/a-$SiN_x$:H/D stack, that has been annealed for 30 min at 450 °C beforehand, was measured. This sample was subject to a new annealing experiment (30 min at 450 °C) during which the lifetime was monitored in real time by *in situ* MPL (see Fig. 7a). Large variations of the lifetime are measured during the heating and cooling phases: $\tau_{eff}$ increases with temperature up to 350 °C and severely drops when the temperature exceeds 350 °C. During the cooling phase $\tau_{eff}$ displays a "symmetrical" behavior, rising rapidly as the temperature drops below 350 °C again, and subsequently decreasing slowly with temperature. During the high temperature plateau (450 °C), the lifetime stays constant. The final lifetime measured by QSSPC is identical to the initial one meaning that the new annealing did not change the passivation of the sample. Consequently, these variations are reversible and are expected to result from two competing phenomena: reversible changes in the overall bulk and surface lifetimes (such as evolution of electron and hole trap capture cross sections) that increase with temperature [33], [54] against Auger or SRH recombinations that are boosted at high temperature (the intrinsic carrier density under thermal equilibrium at 450 °C being around $4 \cdot 10^{16}$ $cm^{-3}$ [55], [56]). Further details can be found in [57]. Another possible explanation could be a temperature dependent steady-state between hydrogen supply, Si-H bond forming and breaking. A similar interpretation of their results was made by Dingemans et al., stating that passivation and dissociation processes take place in parallel, leading to a temperature-dependent equilibrium defect density [12], [58], [59]. Therefore, these variations are not related to the studied hydrogenation process.

Fig. 7b shows the evolution of the lifetime during an annealing at 450°C for 30 min on samples with nc-$SiC_x$(p) and nc-$SiC_x$(n) layers capped with an a-$SiN_x$:H/D layer (as-deposited samples). Both samples display a similar behavior. At the beginning of the annealing step, the lifetime is very low and gradually increases during the temperature plateau at 450 °C until it saturates after 20 minutes. The second part of the graph (cooling phase) is similar to the one shown in Figure 7a. This can be interpreted as follows: at the

beginning, the lifetime is limited by the bulk defects formed during the firing step, thus preventing the emergence of the first lifetime "peak" observed in Fig 7a. At 450 °C, the lifetime increases exponentially, which is consistent with the progressive hydrogenation of the bulk defects, until it saturates when the bulk is completely passivated. At that point, the lifetime is still low (around 250 µs) since it is limited by Auger and SRH recombinations due to the high temperature.

**Commented [LMJ11]:** Pere Roca: Is it exponential ?

**Commented [LMJ12R11]:** It seems to be. At least I can fit it nicely with the formula $\tau_{eff} = [1/\tau_{end} + A \cdot \exp(-t/\tau_{reac})]^{-1}$

In this setup, the hydrogenation seems to take longer than in the previous hotplate annealing experiments. This is most likely due to differences in the heating process. In the case of MPL, the samples are heated in a reactor, which heats up relatively slowly (~30 °C/min), while in the case of hotplate treatment, the samples are put directly on the hotplate pre-heated to 450 °C and thermalize within ~6 s. However, the curves measured by MPL can be fitted with the same formula as the ones from the hotplate experiment, indicating that a similar mechanism is at work. Doing so yields $\tau_{reac}$ = 2.37 min and $\tau_{reac}$ = 2.92 min for the samples with nc-SiC$_x$(p) and nc-SiC$_x$(n), respectively. The passivation thus seems slightly faster for samples with a p-type layer, but otherwise the behavior is similar.

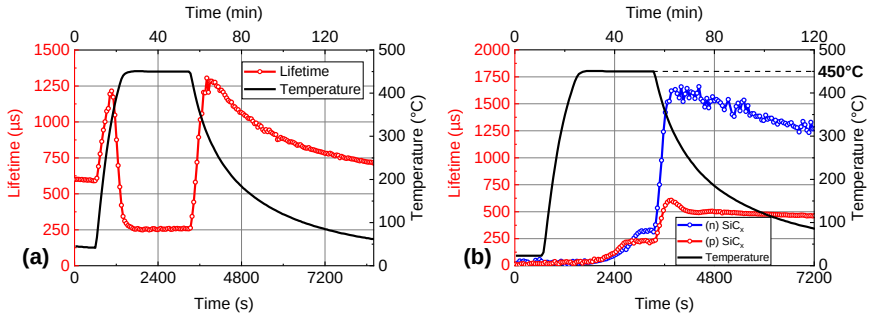


**Fig. 7**: (a): MPL measurement of lifetime (at an excess carrier density of $\mathbf{1 \cdot 10^{15}\ cm^{-3}}$) of a sample featuring nc-SiC$_x$(p) and having already been hydrogenated previously. (b): MPL measurement as function of time during hydrogenation process. Two samples are represented, featuring nc-SiC$_x$(p) and nc-SiC$_x$(n) layers, in order to compare their kinetics.

### 3.4. Hydrogenation with a-SiN$_x$:H/D on front side only

The saturation of $\tau_{eff}$ indicates that more than enough hydrogen is supplied by the a-SiN$_x$:H/D reservoir layers. Moreover, hydrogen was reported to diffuse quickly through c-Si [60]. Therefore, hydrogenation with the a-SiN$_x$:H/D layer on only one side of the wafer was investigated (see Fig. 8a). Note the the samples of this experiment featured interfacial oxides grown by UV-O$_3$ treatment. The possibility to diffuse hydrogen from a front reservoir layer, through the wafer, to the back surface has been reported in literature [61]–[63]. Such an approach might be of interest, as it would simplify the production process of high efficiency solar cell architectures featuring a front a-SiN$_x$:H layer as anti-reflective coating, but no such layer on the rear side [2]. As shown in Fig. 8b, the lifetime saturates at ~700 µs (corresponding to iV$_{OC}$ values ~705 mV) after about 1 hour of hotplate treatment and remains constant for at least 8 hours. Samples from the same experiment, that had an a-SiN$_x$:H/D reservoir layer on both sides, reached lifetimes of ~1300 µs (corresponding to iV$_{OC}$ values ~718 mV). Moreover, none of these samples displayed ring shapes in PL measurements performed after hydrogenation. These results indicate that the hydrogenation of both c-Si/SiO$_x$ interfaces, as well as the bulk, occurs also with the hydrogen source on only one side of the wafer, although to a lower level than with a-SiN$_x$:H/D on both sides.

In order to quantify the passivation of the rear side, the back surface recombination velocity was computed, applying the method presented by Sproul et al. [64], and assuming that the surface recombination velocity at the front side is equal to the one obtained on symmetrical samples with a-$SiN_x$:H/D layer on both sides. As the calculation requires the bulk lifetime, which in our case changes over the course of the process (as shown above), only a lower limit is given, based on the assumption of $\tau_{bulk}$ = 3 ms after hydrogenation (as measured in Fig. 2a for the sample after $SiC_x$(p) deposition); thus, one obtains $S_{front}$ = 6.4 cm/s and $S_{back}$ = 23.6 cm/s. However, it is unlikely that the bulk passivation is as good for a single side hydrogen source than for the case with a-$SiN_x$:H/D on both sides, while the back surface passivation is not. Assuming $S_{front}$ = $S_{back}$ = 6.4 cm/s, one obtains $\tau_{bulk}$ = 1.036 ms. Hence, it is likely that the value of $\tau_{bulk}$ is somewhere in between 1 and 3 ms, while $S_{back}$ lies between 6 and 24 cm/s.

Finite elements simulations, shown in Fig. 8c, indicate that at 450 °C hydrogen can diffuse through the whole wafer in less than a minute, indicating that the hydrogenation process is not diffusion limited. A possible candidate for the factor limiting the hydrogenation is the available hydrogen supply. For these simulations, a Wolfram Mathematica script was written, using the diffusion coefficients given by Carlson et al. [60] for the 30 nm thick nc-$SiC_x$(p) layer and the 280 µm thick c-Si wafer, and those given by Tuttle [65] for the 1.2 nm thick $SiO_x$ layer. For the initial conditions, a hydrogen concentration of $1.14 \cdot 10^{22}$ $cm^{-3}$ in the a-$SiN_x$:H/D layer was used, as has been measured by Elastic Recoil Detection Analysis (ERDA). For the other layers and the bulk, a concentration of $1 \cdot 10^{16}$ $cm^{-3}$ was used, as different levels within the layers or lower concentrations in the bulk could no longer be solved by the script. Note also that the diffusion coefficient used for the nc-$SiC_x$(p) layer was the one for amorphous silicon ($5.77 \cdot 10^{-13}$ $cm^2/s$), which is lower than what is expected for a nano-crystalline layer, and still results in very rapid diffusion of hydrogen from the front source layer to the back side.

SIMS measurements on the rear side, shown in Fig. 8d, revealed the presence of hydrogen in the rear layers, but surprisingly no trace of deuterium could be found, neither after 30 min of diffusion, nor after 2 hours, even though it was incorporated into the a-$SiN_x$:H/D reservoir layer too. Deuterium has a 1.41 times lower diffusion coefficient than hydrogen [60], but is otherwise expected to behave similarly to hydrogen; and in our previous studies, both hydrogen and deuterium were found to diffuse from the a-$SiN_x$:H/D reservoir layer into the sample [14], [66]. Moreover, Mathematica simulations of deuterium diffusion showed results very similar to those of hydrogen. Thus, the absence of deuterium and/or the origin of the observed hydrogen remains an open question and further investigations are needed in order to fully understand the mechanisms at work.

Commented [LMJ13]: HT643, simulations

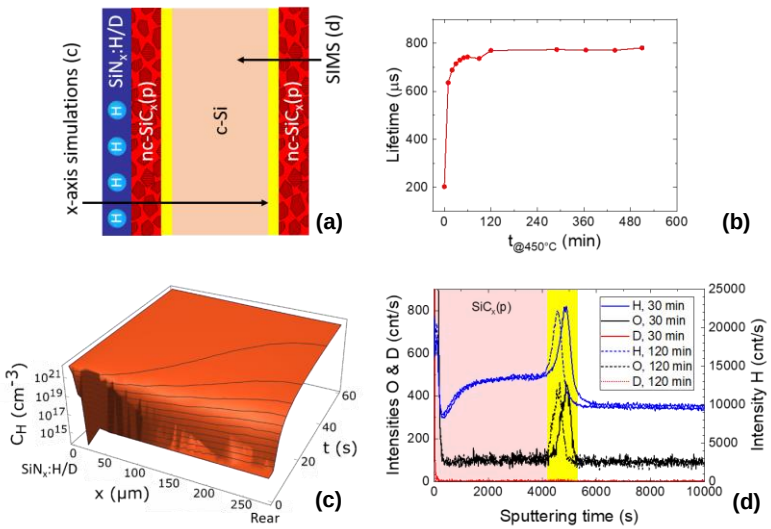


**Fig. 8**: (a) Schematic illustration of the processed samples. The arrows represent the cross sections along which the simulations and SIMS measurements were performed. (b): Lifetimes (at MCD of $\mathbf{1 \cdot 10^{15} cm^{-3}}$) measured at various time intervals during the hydrogenation process, showing the evolution of passivation with time spent on the hotplate, for a sample featuring an a-$SiN_x$:H/D reservoir layer on the front side only. (c) Simulated hydrogen concentrations, across the whole wafer and as a function of time, during diffusion at 450°C from a single side a-$SiN_x$:H/D hydrogen source. (d) SIMS profiles of O, H and D at the back surface. The area highlighted in yellow indicates the $SiO_x$ layer, while the area highlighted in red to the left indicates the nc-$SiC_x$(p) layer.

Kinetics experiments were also performed on these samples, using wafers of different doping types and resistivities, as well as nc-$SiC_x$ layers deposited in different tools. The results in Fig. 9 show that the kinetics are significantly slower than in the previous case with a-$SiN_x$:H/D layers on both sides of the wafer, providing a further indication that the process is likely limited by the supply of hydrogen. Moreover, the doping type of the wafer seems to play a major role for the hydrogenation kinetics, with $\tau_{reac}$ ~ 5 min for p-type wafers, against $\tau_{reac}$ ~ 2.5 min for n-type wafers capped with identical layers. As stated earlier, the wafer doping influences the charge state of diffusing hydrogen atoms [51], which in turn affects the diffusivity of these atoms as well as the efficiency of the chemical passivation process [52], [53]. However, the reported values indicate faster diffusion in p-type silicon than in n-type, whereas we observe faster passivation using n-type wafer. A possible explanation would be that the type and concentration of these defects varies with the wafer doping.

Regarding the various nc-$SiC_x$ layers, the interpretation is complicated, as they differ not only in doping, but also in thickness, and most likely in crystallinity, all of which might impact the flow of hydrogen through these layers. Moreover, in the case of charged hydrogen atoms, electric fields built up at the interfaces might also influence the kinetics and distribution of hydrogen [67]. Further investigations are required to elucidate the mechanisms at work. Nevertheless, one results stands out: The thicknesses measured by ellipsometry for the nc-$SiC_x$(p) layers deposited in the Kai-M, the nc-$SiC_x$(p) layers deposited in the Octopus, and the nc-$SiC_x$(n) layers in the Octopus, were ~41 nm, ~25 nm and ~11 nm, respectively. The corresponding $\tau_{reac}$ on 2 Ω·cm p-type wafers are 5.17 min,

2.33 min and 0.54 min. The last value is to be taken with care, as the lifetime values were low and hence the fit less trustworthy. Nevertheless, the trend indicates slower hydrogenation for thicker layers, which was to be expected, as hydrogen has a much lower diffusivity in these still partially amorphous layers than in crystalline silicon [60], turning them into a significant diffusion barrier, despite thicknesses below 50 nm. This conclusion is further supported by the fact that samples without nc-$SiC_x$ layer consistently displayed slightly faster hydrogenation (not shown here).

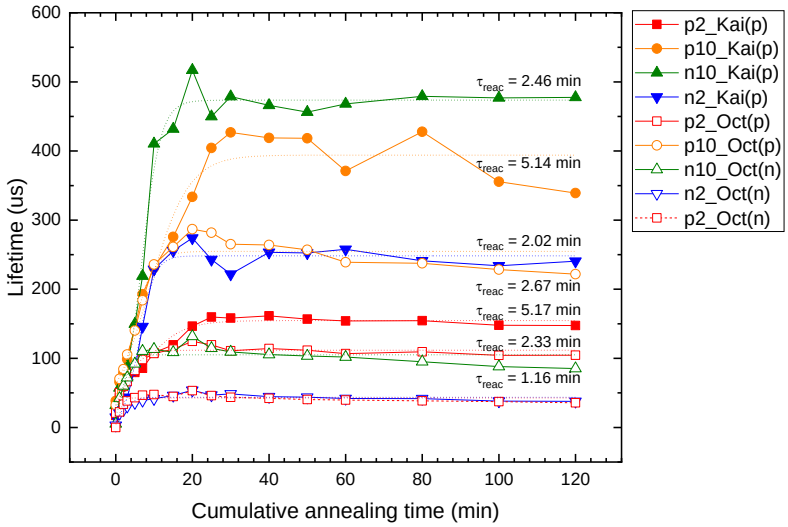


**Fig. 9**: Lifetimes (at MCD of $\mathbf{1 \cdot 10^{15} cm^{-3}}$) measured at various time intervals during the hydrogenation process, showing the evolution of passivation with time spent on the hotplate, for samples featuring an a-$SiN_x$:H/D reservoir layer on the front side only. The dashed lines give the fits according to $\boldsymbol{\tau_{eff} = [1/\tau_{end} + A \cdot \exp(-t/\tau_{reac})]^{-1}}$. In the legend, the first part gives details about the wafer (p- or n-type, 2 or 10 Ωcm), and the second part about the $SiC_x$ layer (deposited in Kai-M or Octopus, p- or n-doped).

When plotting the linearized lifetime curves of QSSPC measurements for this kinetics experiment, one observes again a linear behavior consistent with the presence of shallow bulk defects (see Fig. 10). In the plot of the residuals, there are apparently three different regimes. The curve before hydrogenation differs significantly from all the other ones, which could indicate that, in this case, the surface passivation is still the main limitation. The curves after 1 to 5 min of hydrogen diffusion overlap, with lifetime values about an order of magnitude higher than the original lifetime, indicating that the observed improvement of the lifetime is linked to the passivation of these shallow bulk defects. The subsequent curves overlap at a slightly higher value, but the reason for this additional improvement after 5 min is unclear.

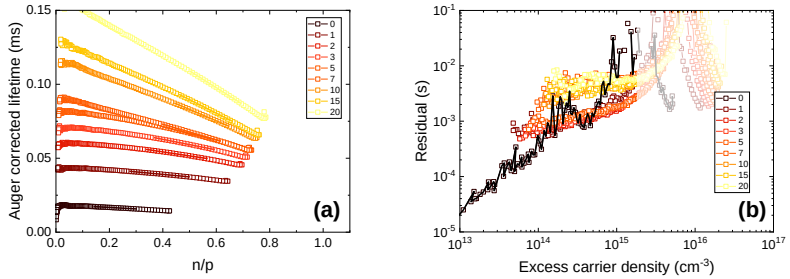


**Fig. 10**: (a) Linearized lifetime curves of QSSPC measurements for various hydrogenation times and fits indicating shallow defects. (b) Residuals after subtraction of Auger and shallow bulk contributions. The legend gives the total time (in minutes) the sample has spent on the hotplate.

## 4. CONCLUSION

The main finding of this work is the fact that firing induces shallow bulk defects within the FZ wafers which can subsequently be passivated with hydrogen, and that these shallow defects limit the kinetics of their hydrogenation process and the ultimately obtainable lifetime. Hence, the passivation potential of these contact structures might be higher than previously reported, since so far they seem to be bulk limited, rather than surface limited. The experimental results indicate a rapid passivation of the surface, taking place in less than 1 min, followed by a slower passivation of the shallow bulk defects. A long thermal pre-treatment of the wafers seems to be a possible way to improve the bulk, accelerating the hydrogenation process.

*In situ* lifetime measurements by MPL were carried out during hydrogenation processes. They revealed that the lifetime improvement displays an exponential increase followed by saturation when the temperature of the sample reaches 450 °C. This plateau is expected to correspond to the best possible bulk defect passivation. No major impact of the nc-$SiC_x$ doping on the evolutions of the lifetime was found, which is consistent with a bulk limited hydrogenation process. Its kinetics seems to be limited by the available hydrogen supply at the c-Si/$SiO_x$ interface, rather than by its diffusion within the bulk of the wafer. Moreover, it is affected by the bulk doping, as well as the $SiC_x$ layer thickness.

Hydrogenation is also possible with an a-$SiN_x$:H/D reservoir layer deposited on 1 side of the wafer only, although resulting in a lower passivation level ($\tau_{eff}$ ~700 µs compared to $\tau_{eff}$ ~1300 µs for symmetrical samples), and slower kinetics ($\tau_{reac}$ ~5 min compared to $\tau_{reac}$ ~0.8 min). The rear surface recombination velocity achieved for UV-$O_3$ $SiO_x$/$SiC_x$(p) stacks with an a-$SiN_x$:H/D layer on the front only most likely lies between 6 and 24 cm/s.

### Acknowledgments

The authors gratefully acknowledge support by the Swiss National Science Foundation (SNF) under Grant no. 200021L_172924/1. The work was co-funded by the Luxembourg National Research Fund (FNR) through grants C18/MS/12661114 (MEMPHIS) and INTER/SNF/16/11536628 (NACHOS), and by the French National Research Agency (Programme d'Investissement d'Avenir – ANR-IEED-002-01). Xavier Niquille is thanked for the wet chemical cleaning of the wafer and the growing of the UV-$O_3$ oxides, as well as Stéphane Ischer (CSEM) for growing of thermal oxides. The authors also thank Brahime El

Adib (LIST) for his technical assistance with SIMS depth profiling, Max Döbeli (ETH Zürich) for ERDA measurements, as well as Hyunjung Park, Ezgi Genç, Sofia Libraro, Joël Spitznagel and Quentin Jeangros for fruitful discussions.

**Conflict of interest**

The authors declare no conflict of interest.

**References**

[1] F. Haase *et al.*, "Laser contact openings for local poly-Si-metal contacts enabling 26.1%-efficient POLO-IBC solar cells," *Sol. Energy Mater. Sol. Cells*, vol. 186, no. May, pp. 184–193, 2018.

[2] A. Richter *et al.*, "Design rules for high-efficiency both-sides-contacted silicon solar cells with balanced charge carrier transport and recombination losses," *Nat. Energy*, vol. 6, no. 4, pp. 429–438, 2021.

[3] Y. Chen *et al.*, "Mass production of industrial tunnel oxide passivated contacts (i-TOPCon) silicon solar cells with average efficiency over 23% and modules over 345 W," *Prog. Photovoltaics Res. Appl.*, p. pip.3180, Jul. 2019.

[4] W. Wu *et al.*, "DEVELOPMENT OF INDUSTRIAL N-TYPE BIFACIAL TOPCON SOLAR CELLS AND MODULES," in *36th European Photovoltaic Solar Energy Conference and Exhibition*, 2019.

[5] J. Bao *et al.*, "TOWARDS 24% EFFICIENCY FOR INDUSTRIAL N-TYPE BIFACIAL PASSIVATING-CONTACT SOLAR CELLS WITH HOMOGENEOUS EMITTER," in *37th European Photovoltaic Solar Energy Conference and Exhibition*, 2020, pp. 160–163.

[6] T. G. Allen, J. Bullock, X. Yang, A. Javey, and S. De Wolf, "Passivating contacts for crystalline silicon solar cells," *Nat. Energy*, pp. 2–3, Sep. 2019.

[7] C. Hollemann *et al.*, "Changes in hydrogen concentration and defect state density at the poly-Si/SiOx/c-Si interface due to firing," *Sol. Energy Mater. Sol. Cells*, vol. 231, no. May, p. 111297, 2021.

[8] C. Hollemann, F. Haase, J. Krügener, R. Brendel, and R. Peibst, "Firing stability of n-type poly-Si on oxide junctions formed by quartz tube annealing," in *IEEE 47th Photovoltaic Specialist Conference (PVSC)*, 2020.

[9] H. E. Çiftpinar *et al.*, "Study of screen printed metallization for polysilicon based passivating contacts," *Energy Procedia*, vol. 124, pp. 851–861, 2017.

[10] A. Ingenito *et al.*, "A passivating contact for silicon solar cells formed during a single firing thermal annealing," *Nat. Energy*, vol. 3, no. 9, pp. 800–808, 2018.

[11] A. Merkle *et al.*, "Atmospheric Pressure Chemical Vapor Deposition of In-Situ Doped Amorphous Silicon Layers for Passivating Contacts," *35th Eur. Photovolt. Sol. Energy Conf. Exhib.*, pp. 785–791, 2018.

[12] G. Dingemans, F. Einsele, W. Beyer, M. C. M. Van De Sanden, and W. M. M. Kessels, "Influence of annealing and Al2O3properties on the hydrogen-induced

passivation of the Si/SiO2interface," *J. Appl. Phys.*, vol. 111, no. 9, 2012.

[13] J. Polzin, B. Hammann, T. Niewelt, W. Kwapil, M. Hermle, and F. Feldmann, "Thermal activation of hydrogen for defect passivation in poly-Si based passivating contacts," *Sol. Energy Mater. Sol. Cells*, vol. 230, no. June, p. 111267, Sep. 2021.

[14] M. Lehmann *et al.*, "Analysis of hydrogen distribution and migration in fired passivating contacts (FPC)," *Sol. Energy Mater. Sol. Cells*, vol. 200, no. June, p. 110018, 2019.

[15] D. Hiller *et al.*, "Kinetics of Bulk Lifetime Degradation in Float-Zone Silicon: Fast Activation and Annihilation of Grown-In Defects and the Role of Hydrogen versus Light," *Phys. status solidi*, vol. 217, no. 17, p. 2000436, Sep. 2020.

[16] F. E. Rougieux, N. E. Grant, C. Barugkin, D. MacDonald, and J. D. Murphy, "Influence of annealing and bulk hydrogenation on lifetime-limiting defects in nitrogen-doped floating zone silicon," *IEEE J. Photovoltaics*, vol. 5, no. 2, pp. 495–498, 2015.

[17] A. Goetzberger, B. Voss, and J. Knobloch, *Sonnenenergie: Photovoltaik*, 2nd ed. Stuttgart: B. G. Teubner, 1997.

[18] W. Von Ammon, "FZ and CZ crystal growth: Cost driving factors and new perspectives," *Phys. Status Solidi Appl. Mater. Sci.*, vol. 211, no. 11, pp. 2461–2470, 2014.

[19] H. Kobayashi, Asuha, O. Maida, M. Takahashi, and H. Iwasa, "Nitric acid oxidation of Si to form ultrathin silicon dioxide layers with a low leakage current density," *J. Appl. Phys.*, vol. 94, no. 11, pp. 7328–7335, 2003.

[20] N. E. Grant and K. R. McIntosh, "Surface Passivation Attained by Silicon Dioxide Grown at Low Temperature in Nitric Acid," *24th Eur. Photovolt. Sol. Energy Conf.*, vol. 30, no. 9, pp. 1676–1679, 2009.

[21] A. Moldovan *et al.*, "Tunnel oxide passivated carrier-selective contacts based on ultra-thin SiO2 layers grown by photo-oxidation or wet-chemical oxidation in ozonized water," in *2015 IEEE 42nd Photovoltaic Specialist Conference (PVSC)*, 2015, vol. 60, no. 1, pp. 1–6.

[22] A. Fukano and H. Oyanagi, "Highly insulating ultrathin SiO2 film grown by photooxidation," *J. Appl. Phys.*, vol. 94, no. 5, pp. 3345–3349, 2003.

[23] A. Moldovan *et al.*, "Simple Cleaning and Conditioning of Silicon Surfaces with UV/Ozone Sources," *Energy Procedia*, vol. 55, pp. 834–844, 2014.

[24] J. G. Fossum and E. L. Burgess, "High-efficiency p+-n-n+ back-surface-field silicon solar cells," *Appl. Phys. Lett.*, vol. 33, no. 3, pp. 238–240, 1978.

[25] J. Snel, "The doped Si/SiO2 interface," *Solid. State. Electron.*, vol. 24, no. 2, pp. 135–139, Feb. 1981.

[26] A. W. Blakers and M. A. Green, "Oxidation condition dependence of surface passivation in high efficiency silicon solar cells," *Appl. Phys. Lett.*, vol. 47, no. 8, pp. 818–820, 1985.

[27] E. Yablonovitch, T. Gmitter, R. M. Swanson, and Y. H. Kwark, "A 720 mV open circuit voltage SiO x : c -Si:SiO x double heterostructure solar cell," *Appl. Phys. Lett.*, vol. 47, no. 11, pp. 1211–1213, Dec. 1985.

[28] G. Nogay *et al.*, "Interplay of annealing temperature and doping in hole selective rear contacts based on silicon-rich silicon-carbide thin films," *Sol. Energy Mater. Sol. Cells*, vol. 173, pp. 18–24, 2017.

[29] D. E. Kane and R. M. Swanson, "Measurement of the emitter saturation current by a contactless photoconductivity decay method," in *Proceedings of the 18th IEEE PVSC*, 1985, pp. 578–583.

[30] R. A. Sinton, A. Cuevas, and M. Stuckings, "Quasi-steady-state photoconductance, a new method for solar cell material and device characterization," in *Conference Record of the Twenty Fifth IEEE Photovoltaic Specialists Conference - 1996*, 1996, pp. 457–460.

[31] A. Cuevas and R. A. Sinton, "Prediction of the open-circuit voltage of solar cells from the steady-state photoconductance," *Prog. Photovoltaics Res. Appl.*, vol. 5, no. 2, pp. 79–90, Mar. 1997.

[32] A. Richter, S. W. Glunz, F. Werner, J. Schmidt, and A. Cuevas, "Improved quantitative description of Auger recombination in crystalline silicon," *Phys. Rev. B - Condens. Matter Mater. Phys.*, vol. 86, no. 16, pp. 1–14, 2012.

[33] A. Desthieux *et al.*, "In Situ Modulated PhotoLuminescence for Process Optimization of Crystalline Silicon Passivation," *Conf. Rec. IEEE Photovolt. Spec. Conf.*, vol. 2020-June, pp. 0964–0968, 2020.

[34] A. R. Chanbasha and A. T. S. Wee, "Ultralow-energy SIMS for shallow semiconductor depth profiling," *Appl. Surf. Sci.*, vol. 255, no. 4, pp. 1307–1310, 2008.

[35] A. Cuevas, T. Allen, J. Bullock, Yimao Wan, Di Yan, and Xinyu Zhang, "Skin care for healthy silicon solar cells," in *2015 IEEE 42nd Photovoltaic Specialist Conference (PVSC)*, 2015, no. 1, pp. 1–6.

[36] N. E. Grant *et al.*, "Permanent annihilation of thermally activated defects which limit the lifetime of float-zone silicon," *Phys. Status Solidi Appl. Mater. Sci.*, vol. 213, no. 11, pp. 2844–2849, 2016.

[37] J. A. T. De Guzman, V. P. Markevich, D. Hiller, I. D. Hawkins, M. P. Halsall, and A. R. Peaker, "Passivation of thermally-induced defects with hydrogen in float-zone silicon," *J. Phys. D. Appl. Phys.*, vol. 54, no. 27, 2021.

[38] J. D. Murphy, K. Bothe, R. Krain, V. V. Voronkov, and R. J. Falster, "Parameterisation of injection-dependent lifetime measurements in semiconductors in terms of Shockley-Read-Hall statistics: An application to oxide precipitates in silicon," *J. Appl. Phys.*, vol. 111, no. 11, 2012.

[39] L. E. Mundt *et al.*, "Spatially Resolved Impurity Identification via Temperature- and Injection-Dependent Photoluminescence Imaging," *IEEE J. Photovoltaics*, vol. 5, no. 5, pp. 1503–1509, Sep. 2015.

[40] W. Shockley and W. T. Read, "Statistics of the Recombinations of Holes and

Electrons," *Phys. Rev.*, vol. 87, no. 5, pp. 835–842, Sep. 1952.

[41] R. N. Hall, "Electron-Hole Recombination in Germanium," *Phys. Rev.*, vol. 87, no. 2, pp. 387–387, Jul. 1952.

[42] Y. Zhu *et al.*, "New insights into the thermally activated defects in n-type float-zone silicon," *AIP Conf. Proc.*, vol. 2147, no. August, 2019.

[43] V. LaSalvia *et al.*, "*Tabula Rasa* for *n* -Cz silicon-based photovoltaics," *Prog. Photovoltaics Res. Appl.*, no. February, pp. 1–8, 2018.

[44] K. F. Kelton, R. Falster, D. Gambaro, M. Olmo, M. Cornara, and P. F. Wei, "Oxygen precipitation in silicon: Experimental studies and theoretical investigations within the classical theory of nucleation," *J. Appl. Phys.*, vol. 85, no. 12, pp. 8097–8111, Jun. 1999.

[45] R. J. Falster, M. Cornara, D. Gambaro, M. Olmo, and M. Pagani, "Effect of High Temperature Pre-Anneal on Oxygen Precipitates Nucleation Kinetics in Si," *Solid State Phenom.*, vol. 57–58, pp. 123–128, Jul. 1997.

[46] C. Allebe *et al.*, "PECVD based layers for improved high temperature industrial Solar cell processes," in *2019 IEEE 46th Photovoltaic Specialists Conference (PVSC)*, 2019, pp. 2196–2199.

[47] N. E. Grant, V. P. Markevich, J. Mullins, A. R. Peaker, F. Rougieux, and D. Macdonald, "Thermal activation and deactivation of grown-in defects limiting the lifetime of float-zone silicon," *Phys. Status Solidi - Rapid Res. Lett.*, vol. 10, no. 6, pp. 443–447, 2016.

[48] V. V. Voronkov, "The mechanism of swirl defects formation in silicon," *J. Cryst. Growth*, vol. 59, no. 3, pp. 625–643, Oct. 1982.

[49] T. Abe and T. Takahashi, "Intrinsic point defect behavior in silicon crystals during growth from the melt: A model derived from experimental results," *J. Cryst. Growth*, vol. 334, no. 1, pp. 16–36, Nov. 2011.

[50] J. Mitchell, D. Macdonald, and A. Cuevas, "Thermal activation energy for the passivation of the n-type crystalline silicon surface by hydrogenated amorphous silicon," *Appl. Phys. Lett.*, vol. 94, no. 16, p. 162102, Apr. 2009.

[51] C. Herring, N. M. Johnson, and C. G. Van de Walle, "Energy levels of isolated interstitial hydrogen in silicon," *Phys. Rev. B*, vol. 64, no. 12, p. 125209, 2001.

[52] P. Hamer, B. Hallam, R. S. Bonilla, P. P. Altermatt, P. Wilshaw, and S. Wenham, "Modelling of hydrogen transport in silicon solar cell structures under equilibrium conditions," *J. Appl. Phys.*, vol. 123, no. 4, 2018.

[53] B. J. Hallam, P. G. Hamer, A. M. Ciesla née Wenham, C. E. Chan, B. Vicari Stefani, and S. Wenham, "Development of advanced hydrogenation processes for silicon solar cells via an improved understanding of the behaviour of hydrogen in silicon," *Prog. Photovoltaics Res. Appl.*, no. October 2019, Jan. 2020.

[54] S. Bernardini, T. U. Naerland, A. L. Blum, G. Coletti, and M. I. Bertoni, "Unraveling bulk defects in high-quality c-Si material via TIDLS," *Prog. Photovoltaics Res. Appl.*,

vol. 25, no. 3, pp. 209–217, Mar. 2017.

[55] S. M. Sze and K. K. Ng, *Physics of Semiconductor Devices*, 3rd Editio. New Jersey: John Wiley & Sons, Ltd, 2007.

[56] C. D. Thurmond, "The Standard Thermodynamic Functions for the Formation of Electrons and Holes in Ge, Si, GaAs , and GaP," *J. Electrochem. Soc.*, vol. 122, no. 8, pp. 1133–1141, Aug. 1975.

[57] A. Desthieux, "Development and characterization of Fired Passivating Contacts for p-type silicon solar cells fabrication," Ecole Polytechnique, 2021.

[58] A. Stesmans, "Interaction of Pb defects at the (111)Si/SiO2 interface with molecular hydrogen: Simultaneous action of passivation and dissociation," *J. Appl. Phys.*, vol. 88, no. 1, pp. 489–497, 2000.

[59] J. H. Stathis, "Dissociation kinetics of hydrogen-passivated (100) Si/SiO2 interface defects," *J. Appl. Phys.*, vol. 77, no. 12, pp. 6205–6207, 1995.

[60] D. E. Carlson and C. W. Magee, "A SIMS analysis of deuterium diffusion in hydrogenated amorphous silicon," *Appl. Phys. Lett.*, vol. 33, no. 1, pp. 81–83, 1978.

[61] B. Nemeth *et al.*, "Effect of the SiO2interlayer properties with solid-source hydrogenation on passivated contact performance and surface passivation," *Energy Procedia*, vol. 124, pp. 295–301, 2017.

[62] H. C. Sio, S. P. Phang, H. T. Nguyen, Z. Hameiri, and D. Macdonald, "Hydrogenation in multicrystalline silicon: The impact of dielectric film properties and firing conditions," *Prog. Photovoltaics Res. Appl.*, vol. 12, no. August, pp. 10–12, 2019.

[63] M. Sheoran *et al.*, "Hydrogen diffusion in silicon from plasma-enhanced chemical vapor deposited silicon nitride film at high temperature," *Appl. Phys. Lett.*, vol. 92, no. 17, pp. 1–4, 2008.

[64] A. B. Sproul, "Dimensionless solution of the equation describing the effect of surface recombination on carrier decay in semiconductors," *J. Appl. Phys.*, vol. 76, no. 5, pp. 2851–2854, 1994.

[65] B. Tuttle, "Energetics and diffusion of hydrogen," *Phys. Rev. B - Condens. Matter Mater. Phys.*, vol. 61, no. 7, pp. 4417–4420, 2000.

[66] S. Pal *et al.*, "Quantification of hydrogen in nanostructured hydrogenated passivating contacts for silicon photovoltaics combining SIMS-APT-TEM: A multiscale correlative approach," *Appl. Surf. Sci.*, vol. 555, no. March, p. 149650, 2021.

[67] F. Kail, A. Hadjadj, and P. Roca i Cabarrocas, "Hydrogen diffusion and induced-crystallization in intrinsic and doped hydrogenated amorphous silicon films," *Thin Solid Films*, vol. 487, no. 1–2, pp. 126–131, 2005.